ELSEVIER

International Journal of Mass Spectrometry 223–224 (2003) 527–538

International Journal of Mass Spectrometry

www.elsevier.com/locate/ijms

Trace gas monitoring at the Mauna Loa Baseline Observatory using Proton-Transfer Reaction Mass Spectrometry

Thomas Karl[a,*], Armin Hansel[b], Tilmann Märk[b], Werner Lindinger[b,✠], David Hoffmann[c]

[a] *National Center for Atmospheric Research, Atmospheric Chemistry Division, P.O. Box 3000, Boulder, CO 80307, USA*
[b] *Institute for Ion Physics, University of Innsbruck, Innsbruck, Austria*
[c] *Climate Monitoring and Diagnostics Laboratory, National Oceanographic and Atmospheric Administration, Boulder, CO, USA*

Received 14 March 2002; accepted 7 June 2002

Abstract

Real time monitoring of volatile organic compounds (VOCs) using a Proton-Transfer Reaction Mass Spectrometer was performed at the Mauna Loa Baseline Station (19.54N, 155.58W) in March/April 2001 (March 23, 2001–April 17, 2001). Mixing ratios for methanol, acetone, acetonitrile, isoprene and methyl vinyl ketone (MVK) plus methacrolein (MACR) ranged between 0.2 and 1.8, 0.2 and 1, 0.07 and 0.2, <0.02 and 0.3, and <0.02 and 0.5 ppbv, respectively. Biomass burning plumes transported from South-East Asia and the Indian Subcontinent across the Pacific influenced part of the measurement campaign. ΔAcetonitrile/ΔCO and Δacetone/Δacetonitrile ratios in these cases were 1.5×10^{-3} to 2.5×10^{-3} and 2–5 ppbv/ppbv, respectively. Overall Asian outflow events were not as frequent during Spring 2001 as in previous years. Methanol did not show significant correlation with CO, acetonitrile, and acetone. The abundance of acetone and CO seemed to be influenced but not dominated by biomass burning and domestic biofuel emissions. (Int J Mass Spectrom 223–224 (2003) 527–538)

Keywords: Trace gas monitoring; Proton-Transfer Reaction Mass Spectrometry; Volatile organic compounds

1. Introduction

Taking into account the expected economic expansion around the Pacific Rim and in the rest of the world, it becomes obvious that pollution can be delivered across the Pacific unless preventative measures are taken. Sharma et al. [1] reported high concentrations of nonmethane-hydrocarbons (NMHC) at Oki Island in Japan and concluded that the East Asia Pacific Rim Region is significantly contaminated from anthropogenic emission transported from the Asian continent by rapid convective movement of air masses. Detailed trajectory analysis by Newell and Evans [2] revealed the seasonal patterns of trans-Pacific transport and the relative importance of Asian and European sources. Polluted air in springtime is typically lifted to the upper troposphere and subsequently transported across the Pacific by the aloft. About 40% of the backtrajectories arriving at the Climate Monitoring and Diagnostics Laboratory (CMDL) monitoring station on Mauna Loa in Spring point westwards and indicate fast 'outflowing' Asian air masses [3]. The pan-Pacific air quality problem has recently been impressively demonstrated by satellite remote sensing images of trans-Pacific aerosol transport in April 1998 and March 2001 [3,4]. MOPITT (Measurements

* Corresponding author. E-mail: tomkarl@ucar.edu
✠ Deceased.

1387-3806/02/$ – see front matter
PII S1387-3806(02)00874-6

of Pollutants in the Troposphere) data revealed substantial export of CO from South-East Asia due to biomass burning activity in this region in Spring 2000 [50]. Singh et al. [5] published results of several abundant oxygenated volatile organic compounds (VOCs) in the Southern and Northern Pacific Hemisphere. The authors concluded that current atmospheric global models are incapable of reproducing ambient mixing ratios of several oxygenated species such as methanol, acetaldehyde, and acetone. The latter three compounds account for more than 65% of the total VOC loading at remote places, such as the Southern Indian Ocean [6,7]. These compounds play an important role in the oxidant balance of the troposphere. Recent evidence suggests that on a global basis acetaldehyde, methanol, and acetone contribute to the "large, diffuse and hitherto-unknown sources of oxygenated organic compounds" seen in the atmosphere [5]. Results from the Indian Ocean Experiment (INDOEX) [6,8–10] demonstrated the importance of biofuel on the Asian Subcontinent. Wisthaler et al. [6] measured the relative abundance of acetonitrile, which represents a selective tracer for biomass burning, to CO suggesting a strong biomass burning source in West India. Similar results were obtained by de Gouw et al. [9]. Results from the Trace P (Transport and Chemical Evolution over the Pacific) experiment show significant pollution off the coast of East Asia and suggest transport of polluted layers into the Pacific. In this paper, we present measurements of methanol, acetonitrile, acetone, isoprene, and methyl vinyl ketone (MVK) plus Methacrolein (MACR), measured by Proton-Transfer Reaction Mass Spectrometry (PTR-MS) at the Mauna Loa Baseline Station during Spring 2001.

2. Experimental

The PTR-MS instrument was situated inside the Keeling building of the CMDL network station on Mauna Loa. Air was pulled through a 10-m manifold (i.d. 10 cm) down from the top of the sampling tower at a pumping speed of ~300 L/s. The pressure inside the manifold was approx. 640 mbar. A 5-m PFA-line (i.d. 1/8 in.) pumped by a diaphragm pump (Pfeiffer, MD4) at a pumping speed of 30 L/min was used to bypass part of this air stream into the PTR-MS sampling line. At its end, another bypass (i.d. 1/16 in.) led 15 sccm into the PTR-MS instrument. The pressure in the 5-m sampling line was reduced down to 400 mbar in order to avoid condensation inside the building, minimize memory effects and assure a fast response time. The overall delay time was less than 5 s. Leak tests were performed with methanol using the fast monitoring capabilities of the PTR-MS.

The Proton-Transfer Reaction Mass Spectrometer has been described in detail elsewhere [11]. H_3O^+ ions are used to ionize VOC via proton-transfer reactions. Since any VOC having a higher proton affinity than water can be ionized by H_3O^+, reported concentrations have to be regarded as upper limits. However, as demonstrated, potential interferences for several VOCs (such as acetonitrile, acetone, and methanol) are either very small (e.g., propanal on mass 59^+) or nonexistent [12,13]. The value for E/N (E being the electric field strength and N the buffer gas density) in the drift tube was kept at about 123 Townsend (Td) high enough to avoid strong clustering of H_3O^+ ions with water and thus a humidity-dependent sensitivity. The sensitivity of the PTR-MS instrument during the Mauna Loa field study was typically on the order of 140 Hz/ppbv (counts per second per ppbv) for acetone and 64 Hz/ppbv for methanol at 2.3 mbar buffer gas pressure with a reaction time of 110 μs and 4 MHz H_3O^+ ions and was obtained from a calibration standard as well as from the theoretical first order reaction:

$$H_3O^+ + VOC \xrightarrow{k} VOCH^+ + H_2O, \quad (1)$$

with k being the reaction rate constant. The detection limit (DL) for compounds investigated in this work was inferred from a signal to noise ratio (S/N) of 2 according to $DL = 2 \times S.D._{blank}/sensitivity$, with $S.D._{blank}$ being the standard deviation of background countrates. For a 10-s integration time, this resulted in detection limits of 54, 6, 8, 10, and 10 pptv for methanol, acetonitrile, acetone, isoprene, and MVK + MACR, respectively. The uncertainty of the concentration measurement was ±20% according to

the specifications of a high concentration standard used for calibration in this work. The PTR-MS was operated in a selective ion mode from March 23, 2001 until April 17, 2001 with a cycling rate of ∼6 min. Reference measurements were taken through a catalytic converter (platinum wool at 430 °C) and were performed about every 30 min to 2 h.

Meteorological data and various other atmospheric components, such as surface CO, CH_4, ozone, and halocarbons were available from continuous long-term measurements being made at the Mauna Loa station. Detailed backtrajectory analysis for Spring 2001 with data from the global ECMWF model were available from CMDL, NOAA (National Oceanic and Atmospheric Administration), and the HYSPLT4 (Hybrid Single-Particle Lagrangian Integrated Trajectory) model [14].

3. Results

3.1. Meteorology

Long-range transport to the Mauna Loa Observatory (MLO) is governed mainly by the interplay of the northeasterly trades, the subtropical jet, the seasonal variation of the quasi-permanent North Pacific subtropical anticyclone and synoptic scale disturbances [15]. In Spring, the anticyclone starts to intensify and migrate northwest, which allows air masses to arrive at the MLO from Asia anticyclonically by curving in the last few days to the south and then west to Hawaii. This typical Spring pattern seemed to have mixed air masses coming from the East Pacific Rim Region south to the observatory on April 13–17. A synoptic scale disturbance shifted the large-scale flow from SE to NE on March 28–29 and caused north easterlies along with elevated pollutant concentrations on the subsequent three days (March 29–31). Spring is characterized by the highest frequency of Asian dust transport to Hawaii [16] and the time of maximum ozone concentrations at the observatory [17]. Indeed, around the second and third week in April 2001, a large dust storm originating from Inner Mongolia passed across the North Pacific and migrated as far as the Mid-West of the US. Backtrajectory analysis suggests that part of these air masses, while crossing the Pacific, were mixed south to the MLO.

The local meteorological patterns at the site are mainly governed by the strength of synoptic-scale or trade winds, the height and strength of the trade wind inversion, the flow of the synoptic winds around the island mountain topography, and the daily heating and cooling cycle on the island. Daytime heating of the island causes a pronounced sea breeze circulation that can force surface air as far as 10 km inland [18]. The warmer land mass results in upslope winds, which typically reach a maximum during the early afternoon and mix boundary layer air up to the site. Afternoon upslope conditions can bring humid air (Fig. 1, panel 1) along with increased concentrations of some locally produced compounds (e.g., from the rain forest and/or ocean) to the observatory. Daytime upslope flow weakens after sunset. Winds become light and variable during the evening transition period. When the mountain has cooled sufficiently, dry downslope flow develops. Nighttime drainage winds dissipate a few hours after sunrise as a result of rapid surface heating. At mid-morning, turbulent upslope flow begins again and cumulus clouds usually form in the saddle region between Mauna Loa and Mauna Kea. At times, when the inversion is weak (approx. +1 °C), upslope winds can carry moist boundary layer air up to the observatory. The thickness of the surface layer at the site is approximately 600 m during upslope and 55 m during downslope conditions [19]. As discussed by Walega et al. [20], ozone exhibits a well-known afternoon minimum (Fig. 1, panel 2) due to low NO concentrations in the marine boundary layer in upslope flow.

3.2. Isoprene and MVK + MACR

Isoprene ($k_{HO}^{298} = 1 \times 10^{-10}$ cm^3/molecule s [21]) and MVK + MACR (averaged $k_{HO}^{298} = 2.7 \times 10^{-11}$ cm^3/molecule s [21]) were monitored at protonated masses 69^+ and 71^+, respectively. These ions showed a very pronounced diurnal cycle with concentrations peaking in the afternoon during upslope conditions.

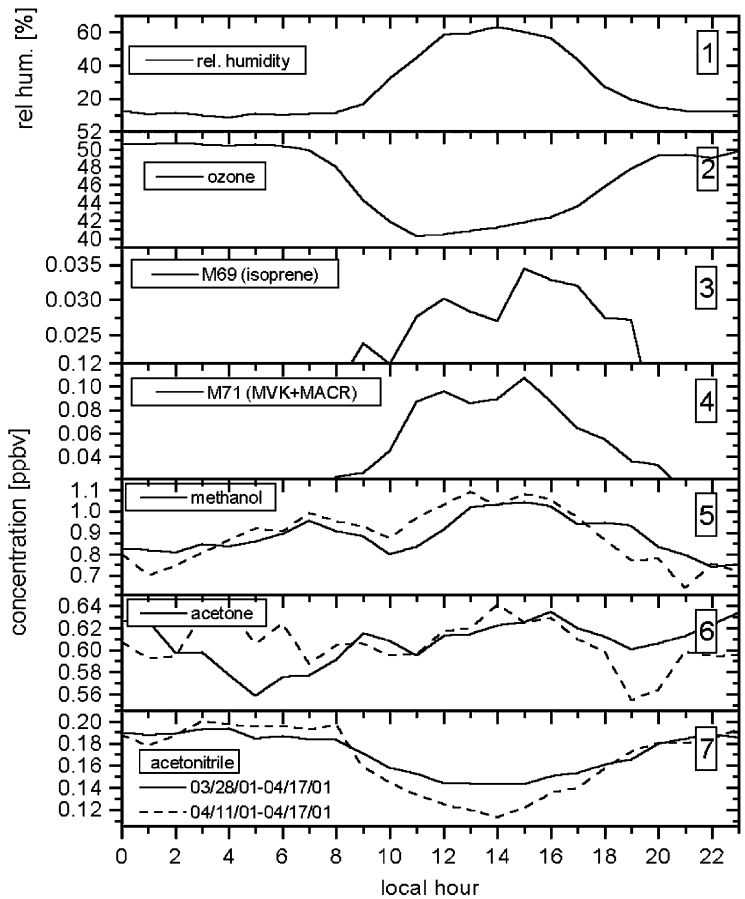

Fig. 1. Averaged diurnal variations of humidity [measured by the $(H_2O)_2H_3O^+$ cluster], ozone, isoprene, MVK + MACR, methanol, acetone, and acetonitrile. Dashed curves in panels 5, 6, and 7 show the averaged diurnal cycle from April 11 till 17.

Nighttime concentrations were close to and below the detection limit <10 pptv. Several potential interferences exhibiting mass 69^+ have been reported [12,13]. For example, unsaturated C_5-alcohols and C_5-aldehydes, which can be released by freezing vegetation, dehydrate partially during proton transfer and thus interfere on mass 69^+. In addition, Harley et al. [22] and Goldan et al. [23] reported that several North American pines release substantial amounts of a C_5-alcohol, 2,3,2-methylbutenol (232-MBO), in a light- and temperature-dependent manner. These interferences cannot be excluded a priori and ambient concentrations for isoprene, therefore, represent an upper limit. Greenberg et al. [24] reported isoprene concentrations around 4–46 pptv during the MLO Photochemistry Experiment 2 (MLOPEX 2). This is close to the mean upslope concentrations (∼30 pptv) observed on mass 69^+ during this study. Fig. 1 (panels 3 and 4) shows the averaged diurnal variation of mass 69^+ (isoprene) and its oxidation products mass 71^+ (MVK + MACR) during the 4-week measurement period. Isoprene is most likely emitted by local vegetation and brought up to the observatory by the diurnal land–sea breeze circulation. Milne et al. [25] reported that isoprene can be produced by phytoplankton and thus emitted by the ocean. Major biogenic interferences can be excluded due to the warm climate (no wound compounds due to temperatures below

freezing) and the local tropical vegetation, which does not accommodate MBO emitting species such as North American pine trees. Helmig et al. [26] investigated the presence of 86 organic species by detailed GC–FID and GC–MS analysis during the MLOPEX 2 study. None of the reported compounds (except isoprene) would contribute to the observed signal on mass 69^+. On an average, two to three times higher mixing ratios of MVK + MACR were observed. Assuming that no significant interferences for the oxidation products of isoprene chemistry exist and taking OH densities on the order of 5×10^6 molecules/cm^3 [27], we derive an average daytime photochemical age between emission and arrival at the observatory of roughly 48 min or a radius of 15 km at an average windspeed of 5 m/s. This is consistent with the idea that upslope winds transport these locally emitted compounds to the site.

3.3. Methanol

Methanol showed concentrations between 0.2 and 1.8 ppbv, close to values (0.5 and 1.6 ppbv) measured by Wisthaler et al. [6] and Warneke and de Gouw [7] in the remote Indian Ocean. Average nighttime concentrations around 800 pptv were a little lower than reported by Singh et al. [5], who measured mean methanol concentrations around 900 pptv in the remote Pacific. The diurnal profile for methanol is shown in Fig. 1 (panel 5). Maximum concentrations were typically observed around 14:00 together with masses 69^+, 71^+, and humidity (measured by the second water cluster $(H_2O)_2H_3O^+$). This suggests that methanol had local sources and was advected to the station by upslope winds. Correlation of methanol and CO was poor with correlation coefficients r between -0.4 and $+0.1$ in general, thus suggesting different origin (except for times when local pollution caused enhanced CO levels at the site by upslope winds, e.g., on April 12, 2001). Methanol to CO ratios are shown in Fig. 2a (panel 3). The straight line (Fig. 2a, panel 3) reflects an average emission factor ($\Delta CH_3OH/\Delta CO = 3.3 \times 10^{-2}$) inferred from burning experiments [28] and was estimated for a 10-day-old air parcel assuming an average HO density (ca. 25% of maximum concentration) of 1×10^6 molecules/cm^3 [27] and a reaction constant with HO of $k_{HO}^{298} = 9.3 \times 10^{-13}$ cm^3/molecule s [21] for methanol and $k_{HO}^{298} = 2.1 \times 10^{-13}$ cm^3/molecule s for CO [21]. This is significantly lower than the observed ratios. Methanol to acetonitrile ratios were significantly higher ($\Delta CH_3OH/\Delta CH_3CN = 5$–$14$) than estimates from biomass burning experiments ($\Delta CH_3OH/\Delta CH_3CN = 2.2 \pm 3$) [28]; our observations, therefore, suggest that the ambient mixing ratios were not greatly influenced by biomass burning. Methanol, an ubiquitous species in the atmosphere, has many sources. Global emission inventories reflect the fact that measurements of this compound are still very scarce [29]. To our knowledge, this was the first time that ambient mixing ratios of methanol were measured on Mauna Loa for a 4-week period. Singh et al. [5] speculate that there might be large primary sources from biogenic emissions. Indeed, first results from several flux studies show high methanol emission rates on the order of several mg/m^2 h (T. Karl, C. Spirig, P. Prevost, C. Stroud, J. Rinne, J. Greenberg, R. Fall, A. Guenther, personal communication). The biogenic source [30] and emission from dead/decaying plant matter [31] of methanol is probably far bigger than secondary production from methane/NMHC oxidation ($2CH_3O_2 \rightarrow CH_3OH + O_2$, 30 Tg/year). Heikes et al. [29] estimate 320 Tg of methanol per year released by biogenic activities. Biomass burning and oceanic sources are thought to be the second major global sources for methanol estimated to account for as much as 22% of the total [29].

3.4. Acetone

Interest in acetone ($k_{HO}^{298} = 1.9 \times 10^{-13}$ cm^3/molecule s [21]) comes from its potential importance in the upper troposphere, where acetone oxidation can produce HO_x radicals ($HO + HO_2$) [32] and thus contribute to ozone formation [33,34]. Acetone can also act as an intermediate sink for NO_x radicals ($NO + NO_2$) by forming peroxy-acetyl nitrate (PAN) and transport these radicals over long distances. Highly variable acetone mixing ratios have been observed

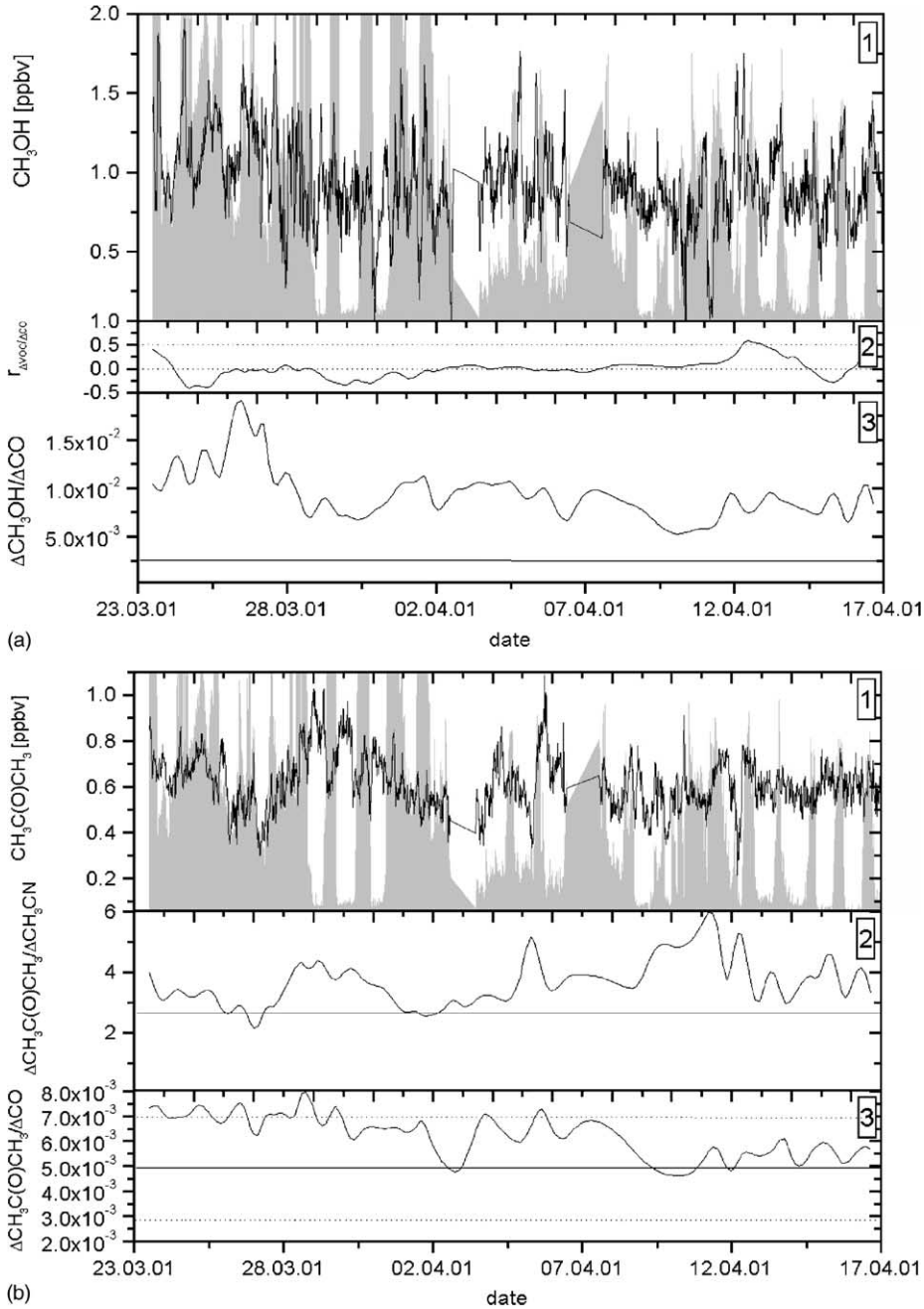

Fig. 2. (a) Panel 1: methanol mixing ratios plotted together with relative humidity (shaded area); panel 2: correlation coefficient *r* between methanol and CO; panel 3: $\Delta CH_3OH/\Delta CO$ ratios, the straight line indicates emission ratios from biomass burning. Correlation coefficients and $\Delta CH_3OH/\Delta CO$ ratios were calculated on an 8-h running mean basis. (b) Panel 1: acetone mixing ratios plotted together with relative humidity (shaded area); panel 2: $\Delta CH_3COCH_3/\Delta CO$ ratios; panel 3: $\Delta CH_3COCH_3/\Delta CH_3CN$ ratios; straight solid lines indicate emission ratios from biomass burning, dashed lines reflect the observed variability. $\Delta CH_3COCH_3/\Delta CO$ and $\Delta CH_3COCH_3/\Delta CH_3CN$ ratios were calculated on an 8-h running mean basis. (c) Panel 1: acetonitrile mixing ratios plotted together with relative humidity (shaded area); panel 2: correlation coefficient *r* between acetonitrile and CO; panel 3: $\Delta CH_3CN/\Delta CO$ ratios, the straight solid line indicates emission ratios from biomass burning, dashed lines reflect the observed variability. Correlation coefficients and $\Delta CH_3CN/\Delta CO$ ratios were calculated on an 8-h running mean basis.

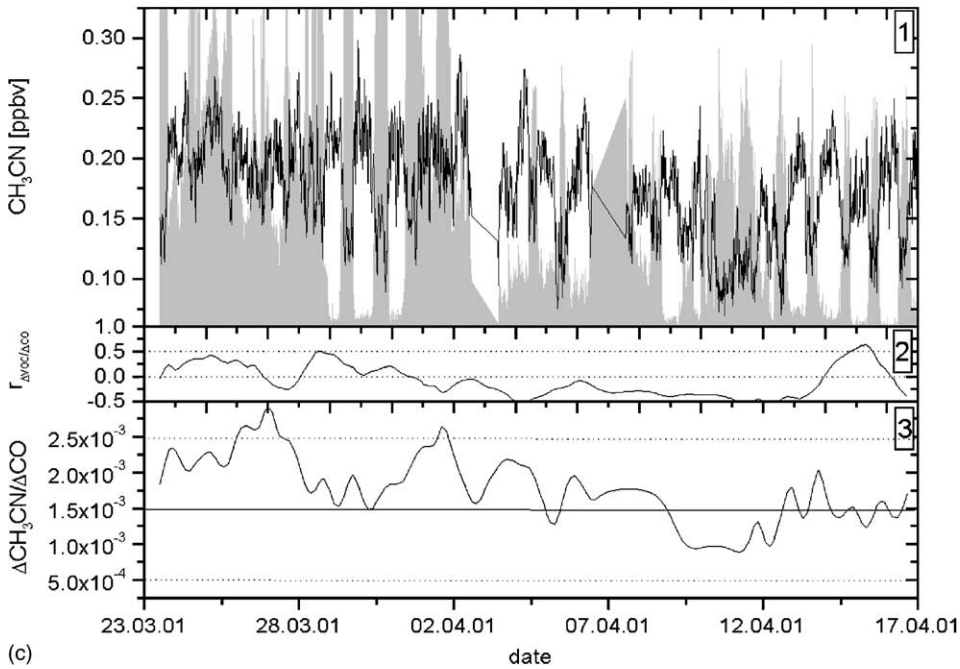

Fig. 2. (*Continued*).

in several previous field studies. Arnold et al. [35] report 3 ppbv in the upper troposphere in the North Atlantic flight corridor, similar enhanced concentrations (2.6 ± 1 ppbv) above the tropical rainforest were published by Pöschl et al. [36], whereas much smaller values around 100 pptv were found in the Pacific region during PEM-West (Pacific Exploratory Mission) [33]. de Gouw et al. [9] report mixing ratios around 500 pptv at altitudes between 4–12 km and 2000 pptv in the lower troposphere (<3 km) during the INDOEX. Clean background concentrations in the pristine boundary layer of the Indian Ocean were observed to be around 450 [6], 350 [7], and 300–800 pptv [37].

In this study, acetone concentrations ranged between 200 and 1000 pptv (Fig. 2b). In contrast to methanol, isoprene, MVK + MACR, and acetonitrile, the averaged diurnal acetone profile (Fig. 1, panel 6) shows no clear trend. Enhanced levels were found during downslope conditions on March 29 (1000 pptv), 30 (800 pptv), and 31 (600 pptv), when 10-day backtrajectories suggest a shift from SE to NE winds. The mean acetone concentration 600 ± 200 pptv was close to values reported by Greenberg et al. [38] during the MLOPEX 2 study. $\Delta CH_3COCH_3/\Delta CO$ ratios (Fig. 2b, panel 3) around 7×10^{-3} with reasonably high correlation coefficients (0.5–0.8) occurred during the first part of the study (March 23–April 2) and were lower ($\Delta CH_3COCH_3/\Delta CO = 5 \times 10^{-3}$) from April 12 onwards. Emission factors from biomass burning would predict values in the range of $4.6 \pm 2.7 \times 10^{-3}$ as indicated by the straight lines in Fig. 2b (panel 3). Correlation coefficients from April 12 onwards show significant variation, with r close to 0 during daytime upslope and r around 0.5–0.8 during nighttime downslope winds; the higher correlation in free tropospheric airmasses can be rationalized by common acetone and CO sources on a larger scale. This is also supported by the cross spectrum of acetone and CO, which shows that most of the positive cross correlation occurs on a time scale around ~5–10 days; wavelet analysis (using the morlet wavelet; $k = 6$) [54] revealed that this mode was dominant throughout almost the whole measurement period; superimposed a second mode on a 1–2 day basis reflected differences

in diurnal variations. Acetonitrile can be regarded as a reasonably good marker for biomass burning. Emission factors for Δacetone/Δacetonitrile have been reported for direct emissions (3.1–5.8 ppbv/ppbv, corrected for a ∼10-day-aged air mass from [28]) and processed plumes (16.2–20 ppbv/ppbv) [39]. Values measured at the MLO are closer to the primary emissions (2–5 ppbv/ppbv) and are shown in Fig. 2b (panel 3). Peak values (8–9 ppbv/ppbv) are typically related to upslope winds and/or poor correlation coefficients. Highest coefficients were observed on March 29 ($r = 0.85$), 30 ($r = 0.5$), and April 14 ($r = 0.5$).

3.5. Acetonitrile

Acetonitrile ($k_{HO}^{298} = 2.2 \times 10^{-14}$ cm^3/molecule s [21]) is thought to be primarily released from biomass burning, although minor contributions from fossil fuel emissions (<6% [40,41]) and biogenic emissions from the breakdown of cyanogenic glycosides similar to HCN might exist [42]. Tropospheric background measurements were reported in the range of 0.075–0.2 ppbv for remote areas and up to 0.4 ppbv in polluted regions during the INDOEX study [6,37]. Warneke and de Gouw [7] measured 122, 154, and 145 pptv in the Southern and Northern Indian Ocean and the Gulf of Aden, respectively. Mixing ratios on ML during Spring 2001 showed minimum concentrations around 70 pptv and peak values up to 300 pptv. This fits well within the previously published concentration range (Fig. 2b, panel 1).

The lifetime according to the reaction with HO radicals is ∼912 days assuming an average HO density of 1×10^6 molecules/cm^3. This does not agree well with observed variability trends [6], which suggests a much lower lifetime. de Laat et al. [10] need an ocean sink assuming dry deposition velocities of 0.01–0.05 cm/s in order to fit modeled acetonitrile data to mixing ratios measured during the INDOEX campaign; however, state that stratosphere/troposphere exchange was not included in their ECHAM (European Center for Medium Range Weather Forcasting) model. Wet deposition of acetonitrile through rain out is currently thought to play a minor role [43,44]. Fig. 3 shows a

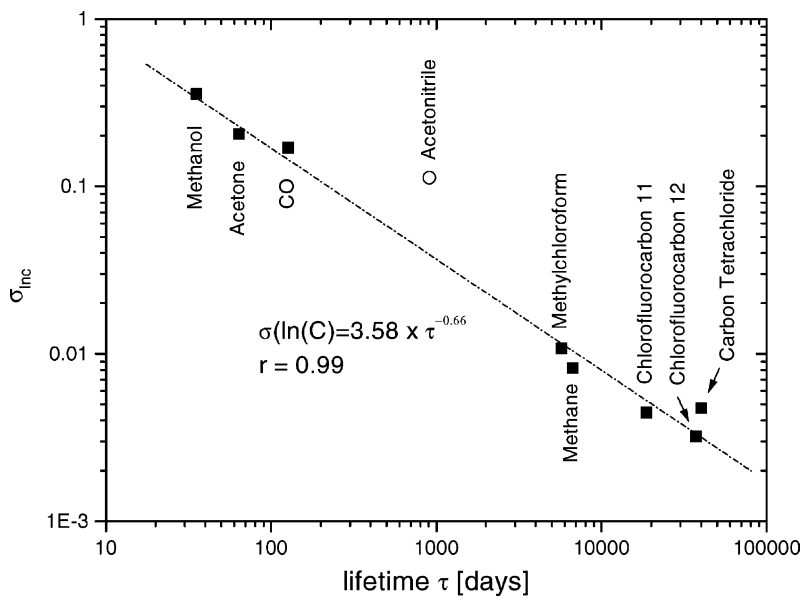

Fig. 3. Variability–lifetime plot of methanol, acetone, acetonitrile, CO, CH_4, methylchloroform, chlorofluorocarbon 11 (F11), chlorofluorocarbon 12 (F12), and carbon tetrachloride. Lifetimes were calculated according to reaction losses due to photolysis and HO radicals. Troposphere Stratosphere Exchange was not considered.

variability–lifetime plot ($s_{\mathrm{lnc}} = A\tau^{-b}$) for some selected long-lived species. The straight line ($r = 0.99$) was fitted through all compounds except acetonitrile. The b factor (0.66) which can be considered as an age factor (the more distant to potential sources the higher) [45,46] is rather large close to values reported during INDOEX (0.4 [7]), PEM-West (0.54 [45]), and LBA-Claire (Large Scale Biosphere-Atmosphere Experiment in Amazonia) (0.64 [47]). The A coefficient (3.58) can be interpreted as a range factor for sampled air mass ages. The observed value (3.58) in Fig. 4 is comparable to those measured during LBA-Claire (4.63) [47] and PEM-West B (4.3) [45] and indicates a rather large age range of sampled pollutants. It is obvious that acetonitrile does not lie within the normal trend ($\tau = 912$ days) if the only considered sink is loss due to reaction with HO radicals. Instead, a lifetime of $\tau = 183$ days seems to be more realistic. The high variability is mainly caused by a pronounced diurnal profile showing lower mixing ratios during upslope (140 pptv) and higher mixing ratios during downslope conditions (200 pptv) (Fig. 1, panel 7). Extreme events caused diurnal variations up to a factor of 2 (March 29–31, April 13–17). These observations seem to support the idea of a missing sink or polluted layers transported by the aloft. Can the pronounced concentration gradient between marine boundary layer (upslope) and free tropospheric air (downslope) be explained by an ocean sink?

Statistical analysis (Fig. 4) of the concentration differences δC in up- and downslope conditions during the Mauna Loa Spring 2001 experiment can be used to test, if the mean gradient seen between the mixed layer and the free troposphere is due to an uptake in ocean water. Using a steady-state approach and the typical marine, convective boundary layer structure, the concentration jump (ΔC) at the top of the boundary layer should be proportional to the ratio of dry

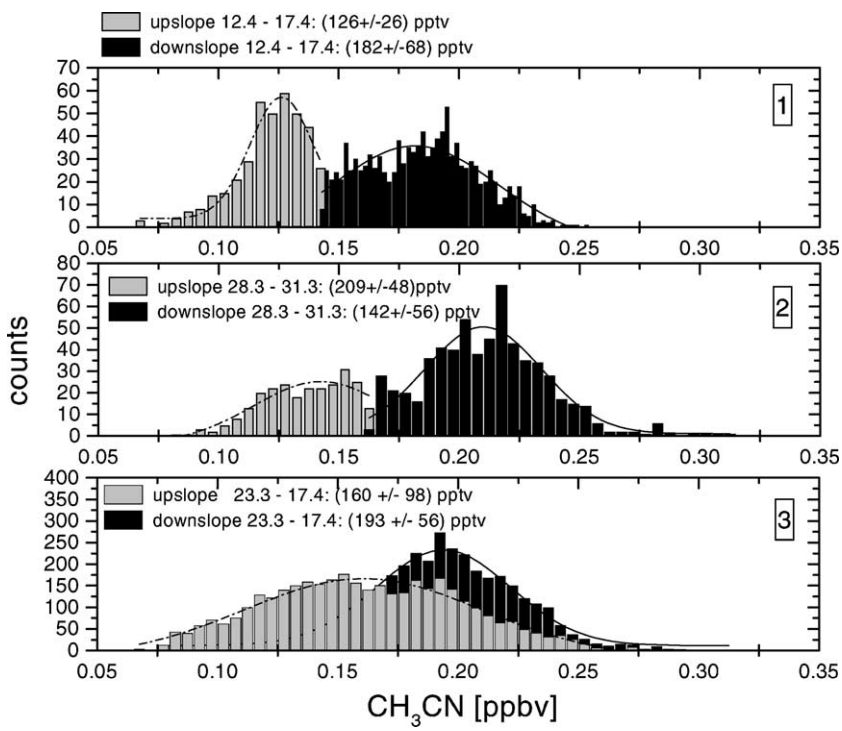

Fig. 4. Acetonitrile concentrations in up-and downslope condititions for the whole MLO Spring 2001 dataset (March 23, 2001–April 17, 2001) and two subsets (March 29, 2001–March 31, 2001 and April 12, 2001–April 17, 2001).

Table 1
Estimated (est.) and experimental (exp.) acetonitrile deposition velocities (v_d) from the literature compared with values obtained from this work (v_e, entrainment velocity in cm/s)

Reference	Reported v_d (cm/s)	Comments	Method
[51]	1×10^{-3} to 3×10^{-3}	Estimation using molecular diffusivities	est.
[52]	0.04–3.7	Adopted from HCN: $v_d \sim u^2$; used in Harvard Global Model	est.
[53]	0.05	Parameterized resistances	est.
[10]	0.01–0.05	New parametrization according to experimental data from the INDOEX 1999	exp.
MLO 2001			v_e
March 28, 2001–April 17, 2001	0.10	Downslope: 19:00–7:00	0.5
March 23, 2001–April 28, 2001 and April 1, 2001–April 14, 2001	0.09	Downslope: 19:00–7:00	0.5
March 28, 2001–March 31, 2001	0.24	Downslope: 19:00–7:00	0.5
April 14, 2001–April 17, 2001	0.17	Downslope: 19:00–7:00	0.5

deposition and entrainment velocities. A simple form of the mixed layer can be written as,

$$\frac{\partial C}{\partial t} + U\frac{\partial C}{\partial x} + \frac{\overline{wc}_{zi} - \overline{wc}_s}{z_i} = S \Rightarrow \frac{\Delta C}{C_{ml}} = \frac{v_d}{v_e} \quad (2)$$

with C (mixing ratio), C_{ml} (concentration in the mixed layer), U (horizontal wind speed), wc_{zi} (entrainment flux), wc_s (surface flux), z_i (boundary layer height), S (chemical loss term), v_d (deposition velocity) and v_e (entrainment velocity). Taking typical values for v_e (0.5 cm/s) measured above the remote ocean [48] and data obtained from this study, we find that the mean gradient could be caused by v_d of 0.1 cm/s for the average concentration profile during the whole study and 0.24 and 0.17 cm/s during March 29–31 and April 13–17, respectively. Table 1 shows a comparison with data for v_d from the literature. Compared to model results from de Laat et al. [10], the mean v_d (0.1 cm/s) is higher by a factor of 2. Two periods (March 29, 2001–March 31, 2001 and April 13, 2001–April 17, 2001) were characterized by a significant enhancement of free tropospheric acetonitrile concentrations resulting in at least five times higher deposition velocities. Even if an uncertainty for entrainment velocities by a factor of two is considered, these enhanced free tropospheric concentrations cannot only be explained by dry deposition in steady state. Remote sensing data (World Fire Web [49]) show that extensive vegetation fires in South-East Asia and the Indian Subcontinent occurred during March and April 2001. Backtrajectories from April 13–16 point westward towards these regions. This supports the idea of air masses influenced by biomass burning which were transported across the Pacific by the aloft within 5–10 days and had not entirely reached an equilibrium with lower marine boundary layer air.

The correlation between CH_3CN and CO is shown in Fig. 2c (panel 3). The ratios range from 1.0 to 2.7×10^{-3}. The period from April 13 on is characterized by $\Delta CH_3CN/\Delta CO$ ratios around 1.5×10^{-3} during downslope conditions falling close to values reported for biofuel ($1.5 \pm 1.0 \times 10^{-3}$, corrected for a ~10-day-aged air mass from [28]). The correlation coefficients $r_{CH_3CN/CO}$ were reasonably high, around 0.6, 0.5, and 0.7 on March 24, March 29–30, and April 14–15, respectively.

4. Conclusion

Continuous ground-based measurements of acetonitrile, acetone, methanol, isoprene, and MVK + MACR made with a Proton-Transfer Reaction Mass Spectrometer were performed at the Mauna Loa Baseline Observatory (CMDL, NOAA) in Spring 2001.

Local influence from the islands caused elevated concentrations for some biogenic and/or oceanic VOCs, such as isoprene, its oxidation products MVK + MACR and sometimes methanol, during afternoon upslope conditions with mean concentrations of 30 pptv, 100 pptv, and 1 ppbv, respectively. Acetonitrile, acetone, and CO were highly correlated on scales between 5 and 7 days during March and the beginning of April (March 23, 2001–April 2, 2001); on March 29–31 specifically, high correlation between these compounds can be rationalized by the back-trajectories suggesting that air masses were passing the Pacific in northern latitudes and shifting 'back' south-east before hitting the US West coast. Influence from both, the Asian continent and the western part of the US is likely. Acetone levels in these cases (0.2–1 ppbv) showed reasonably high correlation with CO ($\Delta CH_3COCH_3/\Delta CO \sim 7 \times 10^{-3}$; $r = 0.8$). Highly variable and enhanced free tropospheric acetonitrile concentrations, a marker for biomass burning and domestic fuel, suggest that the site was partly influenced by biomass burning activities. Detailed backtrajectory analysis showed that between April 13 and 17 air masses from South-East Asia and the Indian Subcontinent were transported across the Pacific within a week resulting in a distinct concentration gradient between marine boundary layer and free tropospheric air. Correlation coefficients between CO and acetonitrile up to 0.7 ($\Delta CH_3CN/\Delta CO = 1.5 \times 10^{-3}$) suggest further that part of the observed CO mixing ratios originated from biomass burning activities such as direct emission and secondary formation in VOC enriched plumes.

Acknowledgements

This paper is dedicated to the memory of our colleague, mentor, and friend Prof. Dr. Werner Lindinger, who lost his life in a tragic accident on Hawaii at the beginning of this experiment in February 2001. Financial support came from the Austrian Fond zur wissenschaftlichen Foerderung (FWF) project 14170, the Bundesministerium für Bildung, Kunst und Forschung, Wien, Austria, the Climate Monitoring and Diagnostics Laboratory (NOAA), and NOAA Grant No. NA06GP0483.

T.K. was also supported by the Atmospheric Chemistry Division and the Advanced Study Program at the National Center for Atmospheric Research. The National Center for Atmospheric Research is sponsored by The National Science Foundation. The authors also want to express thanks to Carsten Warneke, Joost de Gouw, and Brian Heikes for sharing unpublished results, Claire Granier and Guy Brasseur for helpful discussions and Russ Schnell, Fred Fehsenfeld, Ray Fall, and Alex Guenther for their support.

References

[1] U.K. Sharma, Y. Kajii, H. Akimoto, Geophys. Res. Lett. 27 (2000) 2505.
[2] R.E. Newell, M.J. Evans, Geophys. Res. Lett. 27 (2000) 2509.
[3] CMDL, NOAA, Annual Meeting, Abstracts, Boulder, 2001.
[4] K.E. Wilkening, L.A. Barrie, M. Engle, Science 290 (2000) 65.
[5] H.B. Singh, Y. Chen, A. Staudt, D. Jacob, D. Blake, B. Heikes, J. Snow, Nature 410 (2001) 1078.
[6] A. Wisthaler, A. Hansel, R.R. Dickerson, P.J. Crutzen, J. Geophys. Res.-Atmospheres, submitted for publication.
[7] C. Warneke, J.A. de Gouw, Atmos. Environ. 35 (2001) 5923.
[8] J. Lelieveld, et al., Science 291 (2001) 1031.
[9] J.A. de Gouw, C. Warneke, H.A. Scheeren, C. van der Veen, M. Bolder, M.P. Scheele, J. Williams, S. Wong, L. Lange, H. Fischer, J. Lelieveld, J. Geophys. Res. 106 (2001) 28469.
[10] A.T.J. de Laat, J.A. de Gouw, J. Lelieveld, A. Hansel, J. Geophys. Res. 106 (2001) 28469.
[11] W. Lindinger, A. Hansel, A. Jordan, Int. J. Mass Spectrom. 173 (1998) 191.
[12] T. Karl, R. Fall, P.J. Crutzen, A. Jordan, W. Lindinger, Geophys. Res. Lett. 28 (2001) 507.
[13] J.A. de Gouw, C. Warneke, T. Karl, G. Eerdekens, C. van der Veen, R. Fall, Int. J. Mass Spectrom. 223–224 (2003) 365.
[14] R.R. Draxler, G.D. Hess, Aust. Met. Mag. 49 (1998) 295.
[15] J.M. Harris, J.D. Kahl, J. Geophys. Res. 99 (1990) 13651.
[16] J.R. Parrington, W.H. Zoller, N.K. Arras, Science 220 (1983) 195.
[17] S.J. Oltmans, H. Levy II, Atmos. Environ. 28 (1994) 9.
[18] T.A. Schroeder, J. Appl. Meteorol. 20 (1981) 874.
[19] B.G. Mendonca, J. Appl. Meteorol. 5 (1969) 533.
[20] J.G. Walega, B.A. Ridley, S. Madronich, F.E. Grahek, J.D. Shetter, T.D. Sauvain, C.J. Hahn, J.T. Merill, B.A. Bodhaine, E. Robinson, J. Geophys. Res. 97 (1992) 10311.
[21] IUPAC, Summary of Evaluated Kinetic and Photochemical Data for Atmospheric Chemistry, Web Version December 2000. Available at: http://www.iupac-kinetic.ch.cam.ac.uk.

[22] P. Harley, V. Fridd-Stroud, J. Greenberg, A. Guenther, P. Vasconcellos, J. Geophys. Res. 103 (1998) 25479.
[23] P.D. Goldan, W.C. Kuster, F.C. Fehsenfeld, S.A. Montzka, J. Geophys. Res. 98 (1993) 1039.
[24] J.P. Greenberg, P.R. Zimmerman, W.F. Pollock, R.A. Lueb, L.E. Heidt, J. Geophys. Res. 97 (1992) 10395.
[25] P.J. Milne, D.D. Riemer, R.G. Zika, L.E. Brand, Mar. Chem. 71 (1995) 237.
[26] D. Helmig, W. Pollock, J.P. Greenberg, P. Zimmerman, J. Geophys. Res. 101 (1996) 14697.
[27] F.L. Eisele, D.J. Tanner, C.A. Cantrell, J.G. Calvert, J. Geophys. Res. 101 (1996) 14665.
[28] R. Holzinger, C. Warneke, A. Hansel, A. Jordan, W. Lindinger, D.H. Scharffe, G. Schade, P.J. Crutzen, Geophys. Res. Lett. 26 (1999) 1161.
[29] G.B. Heikes, W. Chang, M.E.Q. Pilson, E. Swift, H.B. Singh, A. Guenther, D.J. Jacob, B.D. Field, R. Fall, D. Riemer, L. Brand, Global Biogeochem. Cycles, in press.
[30] R. Fall, A.A. Benson, Trends Plant Sci. 9 (1996) 296.
[31] C. Warneke, T. Karl, H. Judmaier, A. Hansel, A. Jordan, W. Lindinger, P.J. Crutzen, Global Biogeochem. Cycles 13 (1999) 9.
[32] H.B. Singh, M. Kanakidou, P.J. Crutzen, D.J. Jacob, Nature 378 (1995) 50.
[33] S.A. McKeen, et al., Geophys. Res. Lett. 102 (1997) 3177.
[34] P. Wennberg, Science 279 (1998) 49.
[35] F. Arnold, V. Bürger, B. Drostefanke, F. Grimm, A. Krieger, J. Schneider, T. Stilp, Geophys. Res. Lett. 24 (1997) 3017.
[36] U. Pöschl, U.J. Williams, P. Hoor, H. Fischer, P.J. Crutzen, C. Warneke, R. holzinger, A. Hansel, A. Jordan, W. Lindinger, H.A. Scheeren, W. Peters, J. Lelieveld, J. Atmos. Chem. 38 (2001) 115.
[37] D. Sprung, C. Jost, T. Reiner, A. Hansel, A. Wisthaler, J. Geophys. Res. 106 (2001) 28511.
[38] J.P. Greenberg, D. Helmig, P.R. Zimmerman, J. Geophys. Res. 101 (1996) 24581.
[39] A. Andreae, et al., Geophys. Res. Lett. 28 (2001) 951.
[40] R. Holzinger, A. Jordan, A. Hansel, W. Lindinger, J. Atmos. Chem. 38 (2001) 187.
[41] H.W. Bange, J. Williams, Atmos. Environ. 34 (2000) 4959.
[42] R. Fall, T.G. Custer, S. Kato, V. Bierbaum, Atmos. Environ. 35 (2001) 1713.
[43] S. Hamm, P. Warneck, J. Geophys. Res. 95 (1990) 20593.
[44] E. Arijs, G. Brasseur, J. Geophys. Res. 91 (1986) 4003.
[45] B.T. Jobson, S.A. McKeen, D.D. Parrish, F.C. Fehsenfeld, D.R. Blake, A.H. Goldstein, S.M. Schauffler, J.W. Elkins, J. Geophys. Res. 104 (1999) 16090.
[46] T. Karl, P.J. Crutzen, M. Mandl, M. Staudinger, A. Guenther, A. Jordan, R.F.W. Lindinger, Atmos. Environ. 35 (2001) 5287.
[47] J. Williams, H. Fischer, G.W. Harris, P.J. Crutzen, P. Hoor, A. Hansel, R. Holzinger, C. Warneke, W. Lindinger, B. Scheeren, J. Lelieveld, J. Geophys. Res. 105 (2000) 20473.
[48] R. Boers, P.B. Krummel, S.T. Siems, G.D. Hess, J. Geophys. Res. 103 (1998) 16637.
[49] http://www.gvm.sai.jrc.it.
[50] http://www.science.sp-agency.ca/J1-MOPITT.
[51] R.P. Schwarzenbach, P.M. Gschwend, D.M. Imboden, Handbook for Environmental Organic Chemistry, Wiley, New York, 1993.
[52] Q. Li, D.J. Jacob, I. Bey, R.M. Yantosca, Y. Zhao, Y. Kondo, J. Notholt, Geophys. Res. Lett. 27 (2000) 357.
[53] M.L. Wesley, Atmos. Environ. 20 (1989) 1293.
[54] C. Torrence, G.P. Compo, Bull. Am. Meteorological Soc. 79 (1997) 61.